Int. J. Mol. Sci. **2015**, *16*, 476-495; doi:10.3390/ijms16010476

OPEN ACCESS
International Journal of
Molecular Sciences
ISSN 1422-0067
www.mdpi.com/journal/ijms

Article

The Effects of Endogenous Non-Peptide Molecule Isatin and Hydrogen Peroxide on Proteomic Profiling of Rat Brain Amyloid-β Binding Proteins: Relevance to Alzheimer's Disease?

Alexei E. Medvedev [1,2,*], Olga A. Buneeva [1], Arthur T. Kopylov [1], Oksana V. Gnedenko [1], Marina V. Medvedeva [3], Sergey A. Kozin [2], Alexis S. Ivanov [1], Victor G. Zgoda [1] and Alexander A. Makarov [2]

[1] Department of Proteomic Research and Mass Spectrometry, Institute of Biomedical Chemistry, 10 Pogodinskaya Street, Moscow 119121, Russia; E-Mails: olbun@yandex.ru (O.A.B.); a.t.kopylov@gmail.com (A.T.K.); oksana_gnedenko@pochta.ru (O.V.G.); asi@icnet.ru (A.S.I.); vic@ibmh.msk.su (V.G.Z.)

[2] Engelhardt Institute of Molecular Biology, Russian Academy of Sciences, Moscow 119991, Russia; E-Mails: kozinsa@gmail.com (S.A.K.); aamakarov@eimb.ru (A.A.M.)

[3] School of Biology, Lomonosov Moscow State University, Moscow 119191, Russia; E-Mail: marmed64@yandex.ru

* Author to whom correspondence should be addressed; E-Mail: professor57@yandex.ru; Tel.: +7-499-245-05-09; Fax: +7-499-245-08-57.

Academic Editor: Charles A. Collyer

Received: 14 October 2014 / Accepted: 16 December 2014 / Published: 29 December 2014

Abstract: The amyloid-β peptide is considered as a key player in the development and progression of Alzheimer's disease (AD). Although good evidence exists that amyloid-β accumulates inside cells, intracellular brain amyloid-binding proteins remain poorly characterized. Proteomic profiling of rat brain homogenates, performed in this study, resulted in identification of 89 individual intracellular amyloid-binding proteins, and approximately 25% of them were proteins that we had previously identified as specifically binding to isatin, an endogenous neuroprotector molecule. A significant proportion of the amyloid-binding proteins (more than 30%) are differentially expressed or altered/oxidatively modified in AD patients. Incubation of brain homogenates with 70 μM hydrogen peroxide significantly influenced the profile of amyloid-β binding proteins and 0.1 mM isatin decreased the number of identified amyloid-β binding proteins

both in control and hydrogen peroxide treated brain homogenates. The effects of hydrogen peroxide and isatin have been confirmed in optical biosensor experiments with purified glyceraldehyde-3-phosphate dehydrogenase, one of the known crucial amyloid-β binding proteins (also identified in this study). Data obtained suggest that isatin protects crucial intracellular protein targets against amyloid binding, and possibly favors intracellular degradation of this protein via preventing formation of amyloid-β oligomers described in the literature for some isatin derivatives.

Keywords: amyloid-β; amyloid-β binding proteins; proteomic profiling; rat brain; isatin; oxidative stress

1. Introduction

The amyloid-β peptide **1**–**42** formed during proteolytic processing of the amyloid precursor protein (APP) is considered as a key player in the development or progression of Alzheimer's disease (AD) and other pathologies associated with the formation of protein aggregates in the central nervous system ([1–8] and many others). Although much attention is paid to formation of extracellular amyloid plaques and protein aggregates as well as to corresponding mechanisms of their toxicity, good evidence exists that intracellular amyloid-β can accumulate intraneuronally and contribute to disease progression [4,9–15]. Results of experiments on transgenic mice indicate that the intraneuronal amyloid-β accumulation precedes plaque formation [16]. This suggests the importance of amyloid-β interaction with particular intracellular targets. Indeed, interaction of amyloid-β with intracellular catalase caused inactivation of this enzyme and accumulation of hydrogen peroxide inside cells [17]. This implies that oxidative stress induced in the cells exposed to amyloid-β may be (at least partially) associated with reduced degradation of intracellular hydrogen peroxide [17].

In the cell, amyloid-beta was found in different intracellular compartments [4]. The latter suggests the possibility of amyloid interaction with a broad range of proteins, which may be thus denominated as amyloid-β binding proteins. Although there are reports on the interaction of amyloid-β peptide with various intracellular proteins (e.g., [17,18]) and development of protocols for affinity isolation of amyloid-β binding proteins [19], the affinity based proteomic profiling of brain proteins interacting with immobilized amyloid-β has not been performed yet. Some previous studies revealed several important intracellular proteins involved in direct interaction with amyloid-β. These include glyceraldehydes-3-phosphate dehydrogenase (EC 1.2.1.12) (GAPDH) [20–22]. This glycolytic enzyme, a classical glycolytic redox sensitive enzyme, exhibits various non-glycolytic functions that are considered to be especially important for progression of various neurodegenerative diseases, particularly AD [23]. GAPDH is considered as a potential target for neuroprotective drugs. GAPDH interacts with isatin, an endogenous indole exhibiting properties of an endogenous neuroprotective molecule [24–27]. Previous studies have also shown that a significant proportion of rat (or mouse) brain proteins specifically interacted with isatin [28–30], are oxidatively modified in various AD models [11,31–33]. This suggests the existence of a possible interrelationship between capacities of at least some redox sensitive brain intracellular proteins to interact with both amyloid-beta and isatin.

Thus, in this study we have investigated proteomic profiles of beta-amyloid binding proteins of rat brain and their changes induced by hydrogen peroxide and/or isatin. The results of proteomic profiling have been validated in a surface plasmon resonance (SPR) based study with purified glyceraldehyde-3-phosphate dehydrogenase.

Data obtained suggest that interaction between amyloid-beta and its crucial intracellular targets may be influenced by (non-peptide) small organic molecules such as isatin and this opens new possibilities in pharmacological prevention of amyloid-beta toxicity.

2. Results

2.1. Proteomic Profiling of Amyloid-Binding Proteins of Intact Rat Brain Homogenate

Loading of cleared Triton X-100 lysates of whole brain homogenate onto the affinity sorbent, amyloid-beta-Affi-Gel 10, followed by wash with 50 mM potassium phosphate buffer, pH 7.4, resulted in adsorption of 10.4% of the total protein applied. The control Affi-Gel 10 lacking the affinity ligand bound not more than 4% of the total protein applied. This suggests that about 6% of homogenate proteins specifically bound to the affinity sorbent. Subsequent elution of adsorbed proteins followed by their proteomic analysis resulted in identification of at least 89 individual intracellular β-amyloid binding proteins specifically bound to the affinity sorbent (Table S1). They have different intracellular localization and functionally, the identified proteins can be subdivided into the following groups (Figure 1): (i) Energy generation and carbohydrate metabolism; (ii) Cytoskeleton formation and exocytosis/trafficking; (iii) Regulation of gene expression, cell division and differentiation; (iv) Signal transduction and regulation of enzyme activity; (v) Antioxidant and protection proteins/enzymes; (vi) Metabolism of amino acids and other nitrogenous compounds; and (vii) Lipid metabolism. It is particularly significant that metabolic consequences of amyloid-beta interaction with some of these proteins (e.g., catalase, cytochrome oxidase) have already been documented and analyzed in the literature [17,18].

In accordance with our previous studies [28–30], among proteins non-specifically bound to the ligand-free control sorbent, we detected only highly abundant rat brain proteins [34]: The cytoskeletal keratins (10, 1, 6A, 14), and the mitochondrial precursor of β-subunit of ATP synthase. Interestingly, most of these proteins bound non-specifically to both Sepharose [29,30] and Affi-Gel. Thirty of eighty nine amyloid-binding proteins (more than 30%) were found to be oxidatively modified/altered either in brains of AD patients or in different experimental models of this disease (Table 1).

Twenty three of eighty nine amyloid-binding proteins (more than 25%) have been identified earlier [28–30] as proteins specifically bound to isatin (indole-2,3-dione), an endogenous indole which has a distinct and discontinuous distribution in the brain and in other mammalian tissues and body fluids [24,25,27]. Some of them undergo oxidative modification in AD (Table 1).

One of these oxidatively modified proteins which also interact with isatin is glyceraldehyde-3-phosphate dehydrogenase (GAPDH) [26].

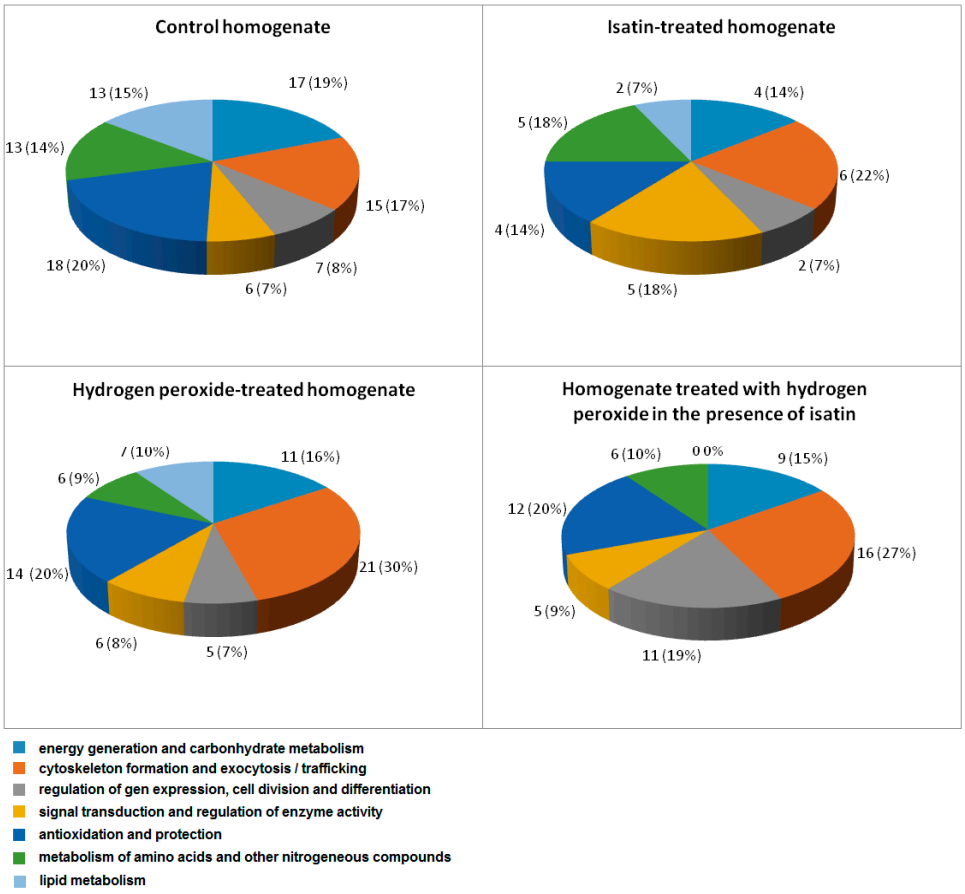

Figure 1. Subdivision of amyloid-binding proteins identified in brain homogenates by their functions: Numbers indicate total number of proteins in each group and numbers in parentheses show the percentage of the total number of identified proteins.

Table 1. Amyloid-binding proteins altered or oxidatively modified in Alzheimer's disease and related pathologies and their experimental models.

No.	Protein Name	Changes in Pathology or Experimental Model	Reference
1	Pyruvate kinase isozymes M1/M2	OM, I	[11,33,35]
2	Actin, cytoplasmic 1	OM, D	[36,37]
3	Heat shock cognate 71 kDa protein	OM	[38]
4	ATP synthase subunit β, mitochondrial	I	[39]
5	Alpha-enolase	OM, I, AALS	[33,35,40,41]
6	Myelin basic protein S	OM	[11]
7	Glutathione *S*-transferase α-2	OM	[11]
8	Dihydropyrimidinase-related protein 2	OM, I, D, AALS	[11,40–42]
9	60 kDa Heat shock protein, mitochondrial	D	[39]
10	Glyceraldehyde-3-phosphate dehydrogenase	OM	[11,33]
11	Fructose-bisphosphate aldolase A	OM	[33]
12	ATP synthase subunit α, mitochondrial	D	[39]
13	Endoplasmin	OM	[33]
14	Peroxiredoxin-1	I	[43]
15	Stress-70 protein, mitochondrial	I	[44–46]

Table 1. *Cont.*

No.	Protein Name	Changes in Pathology or Experimental Model	Reference
16	Retinol-binding protein 4 OS	D	[47]
17	78 kDa Glucose-regulated protein	OM, AALS	[33,41]
18	Peroxiredoxin-2	OM, I	[33,43,48]
19	Glutamine synthetase	OM, I	[11,40]
20	Glutathione *S*-transferase P OS	OM	[11]
21	Glutamate dehydrogenase 1, mitochondrial	OM, AALS	[33,41]
22	Heat shock protein HSP 90-α	I	[49]
23	Spectrin α chain, non-erythrocytic 1	OM	[11]
24	Phosphoglucomutase-1	OM	[32]
25	Synaptotagmin-1	D	[44,50]
26	Phosphatidylethanolamine-binding protein 1	I	[51]
27	Calmodulin	D, AALS	[41,52]
28	Protein disulfide-isomerase	AALS	[41]
29	Superoxide dismutase [Mn]	OM	[53]
30	Tubulin α-1A chain	OM	[32]

I—Increased, D—Decreased, OM—Oxidatively modified, AALS—Altered affinity to lectin sorbents.

2.2. The Effects of Hydrogen Peroxide and Isatin on the Interaction of Glyceraldehyde-3-phosphate Dehydrogenase (GAPDH) with Immobilized Amyloid-β and Actin

The injection of highly purified GAPDH to the biosensor flow cell with immobilized amyloid-β caused a clear concentration-dependent response of the biosensor signal (Figure 2). Its magnitude and shape differed both in the case of intact and oxidized GAPDH and also in the case of the same manipulations with the biosensor flow cell containing immobilized actin, used as a control. This obviously reflects different modes of intact and oxidized GAPDH interaction with immobilized amyloid-β and actin. In order to elucidate affinity of these interactions we have determined K_d values for the complexes of intact and oxidized GAPDH with immobilized amyloid-β and actin.

The calculated K_d value for the GAPDH amyloid-β complex of 0.22 ± 0.02 μM was in the range of K_d values for GAPDH complexes with actin reported in the literature [54]. In our experimental conditions GAPDH affinity to amyloid beta was even higher than to actin (the K_d value of 1.22 ± 0.2 μM, $p < 0.01$ *versus* the K_d value for GAPDH binding to amyloid-β) (Figure 2). Addition of the GAPDH cofactor, NAD (oxidized nicotineamide adenine dinucleotide) (0.01–5 mM), did not influence the behavior of the biosensor response implying lack of any influence of NAD (at least at physiological concentrations) on GAPDH binding to amyloid-β (data not shown), while 0.1 mM isatin decreased this binding and increased the K_d values (Figure 3).

In accordance with previous studies [54], GAPDH oxidation with 70 μM H_2O_2 was accompanied by a dramatic (more than 15-fold) decrease in catalytic activity of this enzyme (from 111 to 6 μmol/min per mg of protein) and also by a dramatic (more than 15-fold) increase in the K_d value for the enzyme interaction with amyloid-β (Figure 3A). This effect was specific for GAPDH interaction with amyloid-β as neither oxidation nor isatin significantly influenced GAPDH interaction with actin,

one of the major cytoskeleton components (Figure 3B). This suggests that oxidative stress and isatin could influence profiles of amyloid-binding proteins in the brain.

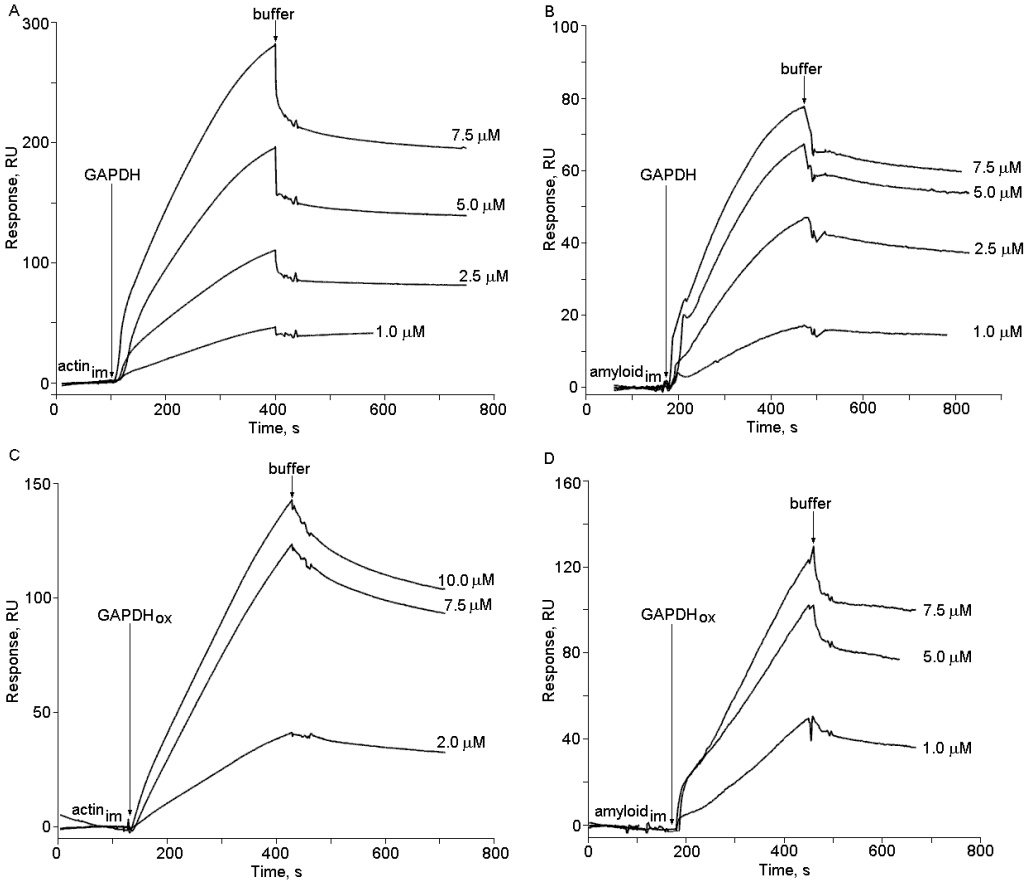

Figure 2. Sensograms of binding of native (**A**,**B**) and oxidized (**C**,**D**) glyceraldehyde-3-phosphate dehydrogenase (GAPDH) to immobilized actin (**A**,**C**) and amyloid-β (**B**,**D**). Arrows indicate onset of injection.

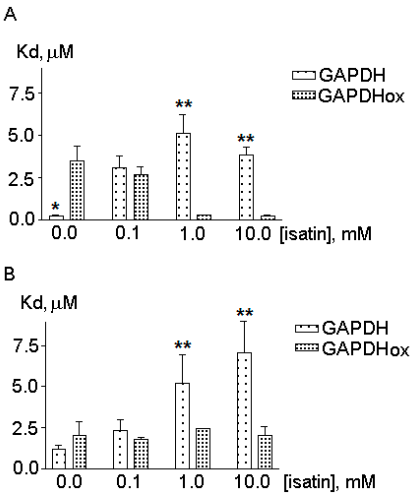

Figure 3. The effect of GAPDH oxidation on K_d values for GAPDH interaction with immobilized actin (**A**) and amyloid-beta (**B**). Data represent mean ± SEM from 3–5 independent experiments. Asterisks show statistically significant differences in K_d values for intact and oxidized GAPDH (* $p < 0.05$; ** $p < 0.01$) evaluated by paired Student's *t*-test.

2.3. Effects of Hydrogen Peroxide and Isatin on Proteomic Profiles of Rat Brain Amyloid-Binding Proteins

Indeed, the presence of 0.1 mM isatin significantly decreased the number of proteins specifically bound to amyloid-β to 28 (Table S2); however, only half of them were common with the group of amyloid-binding proteins of intact brain homogenate.

Induction of oxidative stress by incubating rat brain homogenates with hydrogen peroxide significantly influenced both the total number of amyloid-binding proteins specifically bound to the affinity sorbent and the profile of identified individual proteins (Table S3). The total number of identified proteins slightly decreased (n = 70) and comparison of the proteomic profiles of control and hydrogen peroxide treated brain homogenates revealed 50 common proteins.

Incubation of rat brain homogenate with hydrogen peroxide and isatin caused a further decrease in the total number of brain proteins bound to amyloid-β as compared with hydrogen peroxide treated brain homogenate (59 *versus* 70) (Table S4). However, the number of proteins coincided in brain homogenates treated with hydrogen peroxide in the absence and in the presence of 0.1 mM isatin were just 23, which is significantly less as compared to control and hydrogen peroxide treated homogenates (Figure 4).

In this context, it should be noted that among four groups of rat brain preparations, only six proteins coincided (Table 2); and only two of them, stress-70 protein and endoplasmin, are known to be oxidized in neurodegenerative diseases in patients and/or corresponding experimental models in animals.

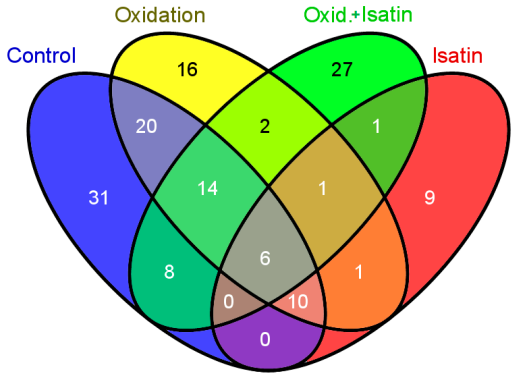

Figure 4. A Venn diagram illustrating the groups comprising the total number of coincided amyloid-binding proteins: control, oxidation, isatin, oxidation in the presence of isatin. Numbers of coincided proteins are shown within intersection areas and numbers outside intersections show proteins specific for each group.

Table 2. Common amyloid-binding proteins for all experimental groups.

No.	Protein Name	Intracellular Localization *	Oxidatively Modified/Altered in AD Brain and Different AD Models **
1	Carbamoyl-phosphate synthase [ammonia], mitochondrial	M	No
2	Betaine-homocysteine *S*-methyltransferase 1	C	No
3	Fructose-bisphosphate aldolase B	C, L, N, ER, CM	No

Table 2. *Cont.*

No.	Protein Name	Intracellular Localization *	Oxidatively Modified/Altered in AD Brain and Different AD Models **
4	Endoplasmin **	ER	Yes
5	Stress-70 protein, mitochondrial **	M	Yes
6	Keratin, type II cytoskeletal 73	C	No

***** Designation of intracellular localization is the same as in other tables; ****** See Table 1 for details and corresponding references.

Thus, it appears that the repertoire of amyloid-beta binding proteins is influenced not only by oxidative stress but also by the presence of low molecular weight substances, which are obviously involved in the regulation of amyloid-β interaction with various subcellular proteins.

3. Discussion

Results of the present study indicate that a large group of intracellular brain proteins can specifically interact with amyloid-β. They belong to different intracellular compartments and different functional groups (Tables S1–S4 and Figure 1).

(Patho)physiological importance of the amyloid-β interaction with some of the identified proteins has been already demonstrated by other authors. For example, catalase inactivation by binding to amyloid-β [17] may explain intracellular accumulation of hydrogen peroxide followed by subsequent development of oxidative stress described in numerous studies. Some cytosolic proteins identified in this study as the amyloid-β binding proteins demonstrate reduced solubility in a transgenic mouse model of Alzheimer-type amyloidosis [16].

More than 30% of amyloid-β binding proteins are oxidized in AD brain and different AD models identified (Table 1). One of these oxidatively-modified proteins is GAPDH. This protein attracts special interest due to its multiple roles related to neurodegeneration and AD [23,55–58].

Being a classical glycolytic enzyme, GAPDH also exhibits various (patho)biological activities (see for review [23,40]) and is a putative target for neuroprotective drugs [26,59,60]. This redox sensitive enzyme can interact with both cytoskeleton components (e.g., actin) [61,62] and aggregate-prone proteins (e.g., amyloid-β) involved in the development and progression of some neurodegenerative disorders such as AD [23,57]. Several studies have demonstrated localization of GAPDH in plaques [55,56]. Binding of this enzyme to the recombinant cytoplasmic domain of β-amyloid precursor protein [20] and immobilized amyloid-β as the affinity ligand [21,63] have shown direct binding of brain GAPDH to both fibrillar and nonfibrillar forms of amyloid-beta peptide **1**–**42**. Although GAPDH also bound to fibrillar crystalline (used as negative control) its coprecipitation with amyloid-β occurred more effectively [21]. Our results of surface plasmon resonance (SPR)-based studies indicate that GAPDH directly binds not only to immobilized amyloid-β but also to actin; however, it also exhibits higher affinity to amyloid-β than to actin. Since physiological concentrations of NAD (cofactor of GADPH) have no influence on GAPDH interaction with amyloid-β, it appears that this interaction does not depend on catalytic properties of this enzyme.

It should be noted that GAPDH represents a good model protein for analysis of interaction of intracellular brain proteins with amyloid-β and the effect of oxidative stress and pharmacologically-relevant compounds on this interaction.

Oxidation of purified GAPDH caused a dramatic decrease in its affinity to amyloid-β as evidenced by a more than 15-fold increase in the K_d value (Figure 3B) for the complex oxidized GADPH immobilized amyloid-β. GAPDH was identified among amyloid-binding proteins after pretreatment of brain homogenate with hydrogen peroxide but it was not detected in the case of intact homogenate pretreated with 0.1 mM isatin (Tables S1 and 3). In this context, it is reasonable to suggest that the K_d values ranging from 2.5 to 3.5 μM (Figure 3) represent the lowest affinity limit, where binding of (oxidized) brain homogenate GAPDH to immobilized amyloid-β was still possible but the presence of 0.1 mM isatin prevented this binding.

As proved by both optical biosensor experiments and proteomic profiling, the presence of 0.1 mM isatin significantly decreased affinity of highly purified GAPDH to amyloid-β immobilized (Figure 3B) on the surface of the biosensor chip and also prevented binding of brain homogenate GAPDH to the affinity sorbent with immobilized amyloid-β as the affinity ligand.

Thus, different interaction behaviors of intact and oxidized purified GAPDH towards amyloid-β immobilized on the biosensor chip is generally consistent with changes in the proteomic profiles of intact and oxidized brain homogenates and the influence of isatin on these protein-amyloid beta interactions.

Isatin is an endogenous indole widely distributed in mammalian brain, peripheral tissues and body fluids [24,25,27]. Its physiological concentrations in blood can exceed 1 μM [64,65]. Although basal tissue concentrations usually vary from 0.1 to 1 μM, in some tissues much higher levels of isatin (40–70 μM) may also occur [27]. It interacts with all known biological targets in a readily reversible manner [24,25,27,29] and demonstration of its *in vivo* interaction with certain biological targets requires employment of special methodological approaches (e.g., [66]). Some experimental evidence exists that isatin may influence interaction of isatin binding proteins with cytoskeletal structures, important for both manifestation and attenuation of neurodegenerative disorders [29].

Mechanism(s), by which isatin decreases the number of proteins bound to the amyloid-β affinity sorbent, still needs clarification. Our results of model experiments with amyloid-β immobilized on the optical biosensor cuvette and (oxidized) GAPDH suggest direct interaction between isatin and amyloid-binding proteins. It appears that isatin competes with amyloid-β for binding to protein targets. By analogy with hydrogen-peroxide induced changes in GAPDH sensitivity to isatin (Figure 2B,C) we suggest that oxidative stress influences protein affinity to isatin and therefore the repertoire of amyloid binding proteins.

Thus, results of our proteomic study indicate that not only oxidative stress *in vitro* but also such non-peptide endogenous compounds as isatin significantly influence the repertoire of brain amyloid-beta binding proteins. The latter suggests that the interaction of amyloid-beta with particular intracellular proteins may be regulated not only by amyloid beta accumulation in various intracellular organelles, and by their redox status, but also by concentrations of endogenous or exogenously administered compounds influencing amyloid-β protein interactions. In this context, it is especially interesting in the present study that in the presence of 0.1 mM isatin only 10% of brain proteins detected coincided with the proteins recently detected as the detergent-insoluble proteins identified

in forebrains of the APPswe/PS1dE9 (line 85) transgenic mice [16]; in the absence of isatin the proportion of coincided proteins exceeded 30%.

The isatin core has been used in the design of various compounds acting as inhibitors of apoptosis, anticonvulsants, and anxiolytics *etc.* [25,67] and administration of isatin improves symptoms of experimental Parkinsonism [68,69]. Studies with [^{3}H]isatin revealed high density of isatin binding in hippocampus, and cortex [28,70,71], *i.e.*, the brain regions affected by amyloid-β deposition in various models of AD. Thus, it appears that the identity of a significant proportion of isatin- and amyloid-binding proteins may have certain biomedical importance, and isatin itself, or its numerous analogues tested in many laboratories for different purposes [27,67,72,73], may be a useful tool for studies of the interaction of amyloid-β and its intracellular targets and possibly as pharmacologically relevant compounds attenuating progression of AD in various experimental models. In this context, it is especially interesting that some recently synthesized isatin-3-arylhydrazones act as rather effective inhibitors of amyloid-β aggregation in model systems [74], while some other isatin derivatives are effective inhibitors of transthyretin fibrillogenesis related to (senile) amyloidosis [75].

Taking into consideration data on the inhibition of aggregation of amyloidogenic proteins by isatin-based compounds, it is reasonable to suggest that endogenous isatin may be an effective neuroprotector at the very beginning of AD. Preventing interaction of amyloid-β with crucial intracellular targets (e.g., catalase, GAPDH, α-enolase *etc.*) isatin promotes their physiological functioning, while maintaining amyloid-β in the monomeric form isatin favors its intracellular degradation (Figure 5).

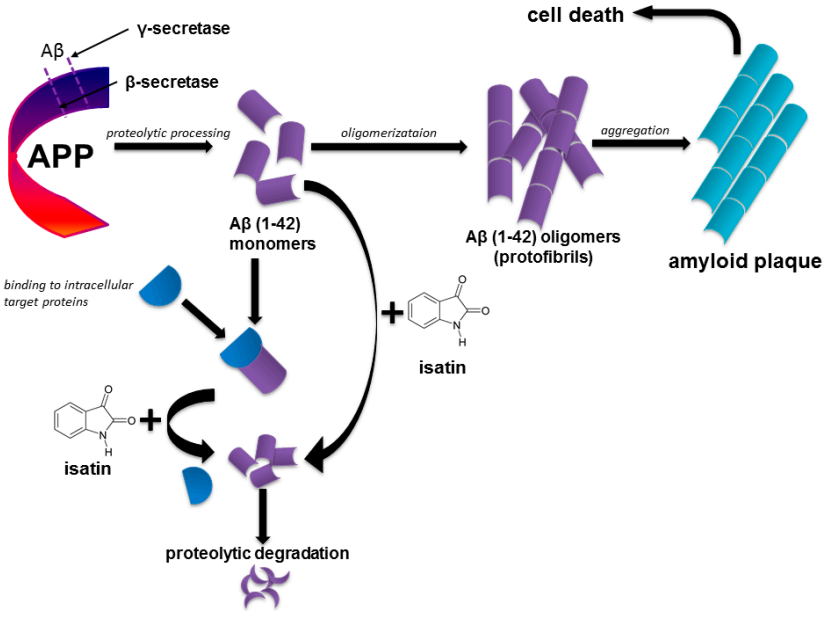

Figure 5. Proposed mechanism of isatin action in prevention of early molecular events leading to development of Alzheimer's disease.

The proposed scenario does not rule out other mechanisms involving direct amyloid-β interaction with its intracellular targets. By analogy with amyloid-beta induced inactivation of catalase [17], it is possible that amyloid-β binding to GAPDH may contribute to energy deficit and impairments in fast axonal transport associated with inhibition/inactivation of this enzyme [76].

4. Experimental Section

4.1. Materials

Acetic acid (sodium salt), boric acid, formic acid, sodium tetraborate, and sodium hydroxide were from Acros Organics (Geel, Belgium). Affi-Gel 10 was purchased from BioRad (Hercules, CA, USA).

Reagents for the Biacore biosensor were obtained from GE Healthcare (Piscataway, NJ, USA). These included HBS-EP buffer (150 mM NaCl, 3 mM EDTA, 0.005% surfactant P20, 10 mM HEPES, pH 7.4); 10 mM acetate buffer, pH 4.0; amine coupling reagents kit, containing 1-ethyl-3-(3-dimethylaminopropyl) carbodiimide hydrochloride (EDC), *N*-hydroxysuccinimide (NHS) and 1 M ethanolamine–HCl, pH 8.5.

All other materials and chemicals including the human amyloid-β protein fragment (**1**–**42**) were from Sigma-Aldrich (St. Louis, MO, USA).

Rabbit muscle GAPDH was purified by the method of Scopes and Stoter [77]. The resulting enzyme preparations (specific activity 110–170 μmol/min per mg of protein as evaluated in the reaction of 3-phosphoglycerate reduction by NADH (reduced nicotinamide adenine dinucleotide) showed one band during electrophoresis in the Laemmli system. Before use, the purified enzyme was kept as an ammonium sulfate suspension at +4 °C for not more than two weeks.

4.2. Animals, Brain Homogenate Preparation and Incubations

Male albino rats (n = 24, 200–250 g) obtained from the Stolbovaya nursery (Russian Academy of Medical Sciences) were used in the experiments performed at least one week after their arrival from the nursery. Animals received a standard laboratory chow and water *ad libitum* and their decapitation was performed between 11.00 and 13.00 h under light ether anesthesia. All procedures conform to the Russian version of the Guide for the Care and Use of Laboratory Animals (Washington, 1996) and have been approved by the Animal Care and Use Committee of the Orekhovich Institute of Biomedical Chemistry issued on 16 June 2014 (identification number: EC3318-2014.2-IBMC).

The brains were immediately dissected and homogenized at a low speed in 0.05 M potassium-phosphate buffer, pH 7.4 (1:3, *w*/*v*), using an Ultra-Turrax T 10 homogenizer as described in [28,29]. In each experiment, the brain homogenates from 2 rats were aliquoted and incubated with 70 μM H_2O_2 in the absence or in the presence of 0.1 mM isatin at 37 °C for 30 min. Control brain homogenates also prepared from 2 rats were incubated during the same period without oxidation in the presence or in the absence of added isatin.

The mild oxidation of GAPDH was performed as described in [54] by incubating GAPDH with 70 μM H_2O_2 for 30 min at 20 °C in 50 mM phosphate buffer, pH 7.4.

*4.3. Immobilization of Amyloid-β Protein Fragment **1**–**42** on Affi-Gel 10*

Amyloid-β protein fragment **1**–**42** (1 mg) dissolved in 250 μL of distilled water was diluted with equal volume of 0.1 M Na-acetate buffer, pH 4.0. In parallel, an Affi-Gel 10 resin (0.5 mL) was washed on a glass filter with 10 volumes of water and 2 volumes of the same buffer. The resin was transferred to the 1.5 mL Eppendorf tubes and the buffer was eliminated by aspiration after

centrifugation of resin slurry at 4000 rpm for 3 min using an Eppendorf centrifuge 5415R (Germany). Amyloid-β protein fragment was added to the mixture (1:1) and incubated at 4 °C overnight at a gentle stirring. The unbound protein fragment was removed by repeated centrifugations (4–5 times) as above in 1 M Tris-acetate buffer, pH 7.0. After addition of the same buffer the resultant suspension (1:1, *v*/*v*) was incubated at 4 °C for 4 h at a gentle stirring. After washing 4–5 times and resuspending in 50 mM potassium phosphate buffer, pH 7.4, containing 0.02% NaN_3, the Affi-Gel 10 resin with the immobilized amyloid-β protein fragment was stored at 4 °C.

All the above-mentioned incubations were performed with the control Affi-Gel, except the addition of amyloid-β protein fragment.

4.4. Affinity Interactions

After incubation at various conditions (see above) homogenates were lysed with 3% Triton X-100 (final concentration) at 4 °C for 1 h, diluted three-fold with 50 mM potassium phosphate buffer, pH 7.4, and centrifuged at 16,000 rpm for 20 min at 4 °C. The resultant supernatant (5 mg of protein/mL) was added to the suspension of the affinity sorbent (Affi-Gel 10 with the immobilized amyloid-β protein) (1:1 *v*/*v*). Bacitracin, aprotinin, and PMSF were added up to the concentrations of 0.005%, 0.01%, and 1 mM, respectively, and the suspension was incubated overnight at 4 °C at a gentle stirring. Such incubation was previously used for the analysis of protein interactions with the recombinant cytoplasmic domain of amyloid-β precursor protein [20]. The same incubations were also performed with the control Affi-Gel 10 without immobilized protein ligands.

After the incubation the sorbent was washed with the same potassium phosphate buffer up to the absence of the protein in the washing (evaluated by baseline at D_{280}) and then packed into the columns (1 × 0.75 mL). Proteins were eluted from the column by 1 M glycine buffer, pH 2.8, containing 150 mM NaCl at a flow rate of 0.5 mL/min. The eluate was concentrated up to 0.200 mL using Amicon Ultra centrifugal filter devices (Millipore, Hessen, Germany) [29]. Proteins were extracted, modified, and digested on filters using the recently published FASP (filter-aided sample preparation) protocol [78].

The peptide samples were analyzed using Ultimate 3000 nano-flow HPLC (Thermo Scientific, Waltham, MA, USA) connected to a LTQ Orbitrap Elite (Thermo Scientific, Waltham, MA USA) mass spectrometer equipped with a Nanospray Flex NG ion source (Thermo Scientific, Waltham, MA USA). Peptide separation was carried out on a RP-HPLC column Zorbax 300SB-C18 (C18 particle size of 3.5 μm, inner diameter of 75 μm and length of 150 mm) using a linear gradient from 95% solvent A (water, 0.1% formic acid) and 5% solvent B (water, 0.1% formic acid, and 80% acetonitrile) to 60% solvent B over 85 min at a flow rate of 0.3 μL/min.

Mass spectra were acquired in the positive ion mode. Data was acquired in the Orbitrap analyzer (Thermo Scientific, Waltham, MA USA) with resolution of 60,000 (*m*/*z* 400) for MS and 15,000 (*m*/*z* 400) for MS/MS scans.

Survey MS scan was followed by MS/MS spectra of the five most abundant precursors. For peptide fragmentation higher energy collisional dissociation (HCD) was used; the signal threshold was set to 10,000 for an isolation window of 2 *m*/*z* and the first mass of HCD spectra was set to 100 *m*/*z*. The collision energy was set to 35 eV. Fragmented precursors were dynamically excluded from

targeting for 60 s. Singly charged ions and ions with undefined charge states were excluded from triggering MS/MS scans.

Protein identification was performed using MASCOT software (www.matrixscience.com). All tandem mass spectra were searched against the SwissProt database (release 2014_02, [79]) The following search parameters were used: Trypsin was used as the cutting enzyme, mass tolerance for the monoisotopic peptide window was set to ±20 ppm, the MS/MS tolerance window was set to ±0.05 Da and one missed cleavage was allowed. Cysteine carbamidomethyl and oxidized methionine were chosen as variable modifications. The criteria of positive identification were set as following: Minimum score of 50, at least three positive identifications from three different runs.

4.5. SPR (Surface Plasmon Resonance) Measurements

GAPDH interaction with immobilized amyloid-beta and actin has been studied using an optical biosensor Biacore 3000 (GE Healthcare, Piscataway, NJ, USA) and the Biacore Control software (GE Healthcare) for instrument operation. All the experiments were performed with the standard optical chips Biacore CM5. Molecular interactions were registered as sensograms representing the records of biosensor signals in resonant units (RU) as time function. The interactions were estimated by subtracting the biosensor signal of a blank flow cell from the signal of the cell with the immobilized ligand or protein.

Covalent immobilization of the proteins (Figure 1) on the sensor chip included surface activation by the 0.2 M EDC/0.05 M NHS mixture and subsequent injection of the solutions (100 μg/mL) of actin or amyloid-β in 10 mM acetate buffer, pH 4.0, at a flow rate of 5 μL/min for 10 and 30 min, respectively. Washing and residual active group inactivations were performed as described in [29].

Protein–protein interactions were monitored by injecting at least five different concentrations of native or oxidized GAPDH (1–10 μM) dissolved in 50 mM potassium phosphate buffer, pH 7.4 (running buffer), at a flow rate of 5 μL/min for 5 min. Each experiment was repeated from three to five times using three different CM5 cuvettes with three different commercial preparations of immobilized amyloid-β peptide. The sensor surface was regenerated after each measurement cycle by washing with 1 M NaCl in the running buffer and 50 mM glycine, pH 9.5, for 0.5 min at a flow rate of 50 μL/min.

Data analysis was performed by applying "Biacore Evaluation v. 4.1" software. To determine the equilibrium dissociation constant ($K_d = 1/K_a$) the equilibrium data were fitted to a single-site model (Equation (1)):

$$R_{eq} = (R_{max} \cdot C \cdot K_a)/(1 + C \cdot K_a) \quad (1)$$

where R_{max} stands for the maximal response; C is the concentration of a protein; R_{eq} is the equilibrium response at a given protein concentration; and K_a is the equilibrium association constant.

4.6. Statistical Analysis

Statistical significance of differences was evaluated by paired Student's *t*-test. Differences were considered as statistically significant at $p < 0.05$.

5. Conclusions

In this study we have investigated profiles of amyloid-binding proteins isolated from control rat brain homogenates and rat brain homogenates treated with hydrogen peroxide (oxidative stress simulation), the small non-peptide endogenous regulator isatin (indole-2,3-dione), and homogenates treated with hydrogen peroxide in the presence of isatin. Proteomic profiling of control rat brain homogenates resulted in identification of 89 individual intracellular amyloid-binding proteins and approximately 25% of them were previously identified as isatin-binding proteins. More than 30% of the amyloid-binding proteins are differentially expressed or altered/oxidatively modified in AD patients. Incubation of brain homogenates with 70 μM hydrogen peroxide significantly influenced the profile of amyloid-β binding proteins and 0.1 mM isatin decreased the number of identified amyloid-β binding proteins both in control and hydrogen peroxide treated brain homogenates. The effects of hydrogen peroxide and isatin have been confirmed in optical biosensor experiments with purified glyceraldehyde-3-phosphate dehydrogenase, one of the known amyloid-β binding proteins also identified in this study. Our results suggest that isatin protects crucial intracellular protein targets against amyloid binding. This effect possibly favors intracellular degradation of this protein via preventing formation of amyloid-β oligomers described in the literature for some isatin derivatives. If such a scenario occurs *in vivo*, it appears that endogenous and/or pharmacological compounds decreasing amyloid-β interaction with numerous amyloid-binding proteins in the brain would be especially effective at early stages of AD, when toxic amyloid-β oligomers have not yet been formed.

Supplementary Materials

Supplementary tables can be found at http://www.mdpi.com/1422-0067/16/01/0476/s1.

Acknowledgments

This work was supported by the Russian Scientific Foundation grant # 14-24-00100.

Author Contributions

Alexei E. Medvedev, Alexis S. Ivanov, and Alexander A. Makarov conceived the study and performed data analysis, Olga A. Buneeva performed affinity based isolation of amyloid-binding proteins and data analysis, Arthur T. Kopylov and Victor G. Zgoda performed mass spectrometry studies and protein identification and contributed with valuable discussion, Oksana V. Gnedenko performed optical biosensor measurements, Marina V. Medvedeva purified glyceraldehyde-3-phosphate dehydrogenase and studied the effect of hydrogen peroxide on catalytic activity of this enzyme. Sergey A. Kozin performed data analysis and contributed with valuable discussions. Alexei E. Medvedev drafted the manuscript. All authors read and approved the final manuscript.

Conflicts of Interest

The authors declare no conflict of interest.

References

1. Schmechel, D.E.; Saunders, A.M.; Strittmatter, W.J.; Crain, B.J.; Hulette, C.M.; Joo, S.H.; Pericak-Vance, M.A.; Goldgaber, D.; Roses A.D. Increased amyloid beta-peptide deposition in cerebral cortex as a consequence of apolipoprotein E genotype in late-onset Alzheimer disease. *Proc. Natl. Acad. Sci. USA* **1993**, *90*, 9649–9653.
2. Saido, T.C.; Iwatsubo, T.; Mann, D.M.; Shimada, H.; Ihara, Y.; Kawashima, S. Dominant and differential deposition of distinct β-amyloid peptide species, $A\beta_{N3}$(pE), in senile plaques. *Neuron* **1995**, *14*, 457–466.
3. Hardy, J.; Selkoe, D.J. The amyloid hypothesis of Alzheimer's disease: Progress and problems on the road to therapeutics. *Science* **2002**, *297*, 353–356.
4. LaFerla, F.M.; Green, K.N.; Oddo, S. Intracellular amyloid-β in Alzheimer's disease. *Nat. Rev. Neurosci.* **2007**, *8*, 499–509.
5. Masters, C.L.; Selkoe, D.J. Biochemistry of amyloid β-protein and amyloid deposits in Alzheimer disease. *Cold Spring Harb. Perspect. Med*. **2012**, *6*, a006262.
6. Mitkevich, V.A.; Petrushanko, I.Y.; Yegorov, Y.E.; Simonenko, O.V.; Vishnyakova, K.S.; Kulikova, A.A.; Tsvetkov, P.O.; Makarov, A.A.; Kozin, S.A. Isomerization of Asp7 leads to increased toxic effect of amyloid-β42 on human neuronal cells. *Cell Death Dis*. **2013**, *4*, e939.
7. Kozin, S.A.; Cheglakov, I.B.; Ovsepyan, A.A.; Telegin, G.B.; Tsvetkov, P.O.; Lisitsa, A.V.; Makarov, A.A. Peripherally applied synthetic peptide isoAsp-Aβ(**1**–**42**) triggers cerebral β-amyloidosis. *Neurotox. Res*. **2013**, *24*, 370–376.
8. Upadhaya, A.; Kosterin, I.; Kumar, S.; von Arnim, C.A.; Yamaguchi, H.; Fändrich, M.; Walter, J.; Thal, D.R. Biochemical stages of amyloid-β peptide aggregation and accumulation in the human brain and their association with symptomatic and pathologically preclinical Alzheimer's disease. *Brain* **2014**, *137*, 887–903.
9. Li, Q.X.; Maynard, C.; Cappai, R.; McLean, C.A.; Cherny, R.A.; Lynch T.; Culvenor, J.G.; Trevaskis, J.; Tanner, J.E.; Bailey, K.A.; *et al.* Intracellular accumulation of detergent-soluble amyloidogenic Aβ fragment of Alzheimer's disease precursor protein in the hippocampus of aged transgenic mice. *J. Neurochem.* **1999**, *72*, 2479–2487.
10. Wirths, O.; Multhaup, G.; Czech, C.; Blanchard, V.; Moussaoui, S.; Tremp, G.; Pradier, L.; Beyreuther, K.; Bayer, T.A. Intraneuronal Aβ accumulation precedes plaque formation in β-amyloid precursor protein and presenilin-1 double-transgenic mice. *Neurosci. Lett.* **2001**, *306*, 116–120.
11. Butterfield, D.A.; Sultana, R.; Poon, H.F. Redox proteomics: A new approach to investigate oxidative stress in Alzheimer's disease. In *Redox Proteomics: From Protein Modifications to Cellular Dysfunction and Diseases*; Dalle-Donne, I., Scaloni, A., Butterfield, D.A., Eds.; John Wiley & Sons Inc.: Hoboken, NJ, USA, 2006; pp. 563–603.
12. Knobloch, M.; Konietzko, U.; Krebs, D.C.; Nitsch, R.M. Intracellular Aβ and cognitive deficits precede β-amyloid deposition in transgenic arcAβ mice. *Neurobiol. Aging* **2007**, *28*, 1297–1306.
13. Reddy, P.H.; Beal M.F. Amyloid beta, mitochondrial dysfunction and synaptic damage: Implications for cognitive decline in aging and Alzheimer's disease. *Trends Mol. Med.* **2008**, *14*, 45–53.

14. Spuch, C.; Ortolano, S.; Navarro, C. New insights in the amyloid-beta interaction with mitochondria. *J. Aging Res.* **2012**, 324968.
15. Wu, Z.; Zhu, Y.; Cao, X.; Sun, S.; Zhao, B. Mitochondrial toxic effects of Aβ through mitofusins in the early pathogenesis of Alzheimer's disease. *Mol. Neurobiol.* **2004**, *50*, 986–996.
16. Xu, G.; Stevens, S.M., Jr.; Moore, B.D.; McClung, S.; Borchelt, D.R. Cytosolic proteins lose solubility as amyloid deposits in a transgenic mouse model of Alzheimer-type amyloidosis. *Hum. Mol. Genet.* **2013**, *22*, 2765–2774.
17. Habib, L.; Lee, M.T.C.; Yang, J. Inhibitors of catalase-amyloid interactions protect cells from β-amyloid-induced oxidative stress and toxicity. *J. Biol. Chem.* **2010**, *285*, 38933–38943.
18. Hernandez-Zimbron, L.F.; Luna-Munoz, J.; Mena, R.; Vazquez-Ramirez, R.; Kubli-Garfias, C.; Cribbs, D.H.; Manoutcharian, K.; Gevorkian, G. Amyloid-β peptide binds to cytochrome C oxidase subunit 1. *PLoS One* **2012**, *7*, e42344.
19. Calero, M.; Rostagno, A.; Ghiso, J. Search for amyloid-binding proteins by affinity chromatography. *Methods Mol. Biol.* **2012**, *849*, 213–223.
20. Schulze, H.; Schuler, A.; Stuber, D.; Dobeli, H.; Langen, H.; Huber, G. Rat brain glyceraldehyde-3-phosphate dehydrogenase interacts with the recombinant cytoplasmic domain of Alzheimer's beta-amyloid precursor protein. *J. Neurochem.* **1993**, *60*, 1915–1922.
21. Verdier, Y.; Földi, I.; Sergeant, N.; Fülöp, L.; Penke, Z.; Janáky, T.; Szücs, M.; Penke, B. Characterization of the interaction between Aβ **1**–**42** and glyceraldehyde phosphodehydrogenase. *J. Pept. Sci.* **2008**, *14*, 755–762.
22. Naletova, I.; Schmalhausen, E.; Kharitonov, A.; Katrukha, A.; Saso, L.; Caprioli, A.; Muronetz, V. Non-native glyceraldehyde-3-phosphate dehydrogenase can be an intrinsic component of amyloid structures. *Biochim. Biophys. Acta* **2008**, *1784*, 2052–2058.
23. Butterfield, D.A.; Hardas, S.S.; Bader Lange, M.L. Oxidatively modified glyceraldehyde-3-phosphate dehydrogenase (GAPDH) and Alzheimer disease: Many pathways to neurodegeneration. *J. Alzheimers Dis*. **2010**, *20*, 369–393.
24. Medvedev, A.E., Clow, A.; Sandler, M.; Glover, V. Isatin–A link between natriuretic peptides and monoamines? *Biochem. Pharmacol.* **1996**, *52*, 385–391.
25. Medvedev, A.; Igosheva, N.; Crumeyrolle-Arias, M.; Glover, V. Isatin: Role in stress and anxiety. *Stress* **2005**, *8*, 175–183.
26. Medvedev, A.; Buneeva, O.; Gnedenko, O.; Fedchenko, V.; Medvedeva, M.; Ivanov, Y.; Glover, V.; Sandler, M. Isatin interaction with glyceraldehyde-3-phosphate dehydrogenase, a putative target for neuroprotective drugs: Partial agonism with deprenyl. *J. Neural. Transm. Suppl.* **2006**, *71*, 195–203.
27. Medvedev, A.; Buneeva, O.; Glover, V. Biological targets for isatin and its analogues: Implications for therapy. *Biologics* **2007**, *1*, 151–162.
28. Crumeyrolle-Arias, M.; Buneeva, O.; Zgoda, V.; Kopylov, A.; Cardona, A.; Tournaire, M.-C.; Pozdnev, V.; Glover, V.; Medvedev, A. Isatin binding proteins in rat brain: *In situ* imaging, quantitative characterization of specific [^{3}H]isatin binding, and proteomic profiling. *J. Neurosci. Res.* **2009**, *87*, 2763–2772.

29. Buneeva, O.; Gnedenko, O.; Zgoda, V.; Kopylov, A.; Glover, V.; Ivanov, A.; Medvedev, A.; Archakov, A. Isatin binding proteins of rat and mouse brain: Proteomic identification and optical biosensor validation. *Proteomics* **2010**, *10*, 23–37.
30. Buneeva, O.A.; Kopylov, A.T.; Tikhonova, O.V.; Zgoda, V.G.; Medvedev, A.E.; Archakov, A.I. Effect of affinity sorbent on proteomic profiling of isatin binding proteins of mouse brain. *Biochemistry (Moscow)* **2012**, *77*, 1326–1328.
31. Butterfield, D.A.; Poon, H.F.; St Clair, D.; Keller, J.N.; Pierce, W.M.; Klein, J.B.; Markesbery, W.R. Redox proteomics identification of oxidatively modified hippocampal proteins in mild cognitive impairment: Insights into the development of Alzheimer's disease. *Neurobiol. Dis.* **2006**, *22*, 223–232.
32. Baraibar, M.A.; Liu, L.; Ahmed, E.K.; Friguet, B. Protein oxidative damage at the crossroads of cellular senescence, aging, and age-related diseases. *Oxid. Med. Cell. Longev*. **2012**, *2012*, 919832.
33. Di Domenico, F.; Pupo, G.; Tramutola, A.; Giorgi, A.; Schininà, M.E.; Coccia, R.; Head, E.; Butterfield, D.A.; Perluigi, M. Redox proteomics analysis of HNE-modified proteins in Down syndrome brain: Clues for understanding the development of Alzheimer disease. *Free Radic. Biol. Med.* **2014**, *71*, 270–280.
34. Witzmann, F.A.; Arnold, R.J.; Bai, F.; Hrncirova, P.; Kimpel, M.W.; Mechref, Y.S.; McBride, W.J.; Novotny, M.V.; Pedrick, N.M.; Ringham, H.N.; *et al.* A proteomic survey of rat cerebral cortical synaptosomes. *Proteomics* **2005**, *5*, 2177–2201.
35. Reed, T.T.; Sultana, R.; Butterfield, D.A. Redox proteomics of oxidatively modified brain proteins in mild cognitive impairment. In *Neuroproteomics*; Alzate, O., Ed.; CRC Press: Boca Raton, FL, USA, 2010.
36. Butterfield, D.A. Amyloid β-peptide (**1**–**42**)-induced oxidative stress and neurotoxicity: Implications for neurodegeneration in Alzheimer's disease brain. A review. *Free Radic. Res.* **2002**, *36*, 1307–1313.
37. Butterfield, D.A. Proteomics: A new approach to investigate oxidative stress in Alzheimer's disease brain. *Brain Res.* **2004**, *1000*, 1–7.
38. Castegna, A.; Aksenov, M.; Thongboonkerd, V.; Klein, J.B.; Pierce, W.M.; Booze, R.; Markesbery, W.R.; Butterfield, D.A. Proteomic identification of oxidatively modified proteins in Alzheimer's disease brain. Part II: Dihydropyrimidinase-related protein 2, α-enolase andheat shock cognate 71. *J. Neurochem.* **2002**, *82*, 1524–1532.
39. Tsuji, T.; Shiozaki, A.; Kohno, R.; Yoshizato, K.; Shimohama, S. Proteomic profiling and neurodegeneration in Alzheimer's disease. *Neurochem. Res.* **2002**, *27*, 1245–1253.
40. Castegna, A.; Aksenov, M.; Aksenova, M.; Thongboonkerd, V.; Klein, J.B.; Pierce, W.M.; Booze, R.; Markesbery, W.R.; Butterfield, D.A. Proteomic identification of oxidatively modified proteins in Alzheimer's disease brain. Part I: Creatine kinase BB, glutamine synthase, and ubiquitin carboxyterminal hydrolase L-1. *Free Radic. Biol. Med.* **2002**, *33*, 562–571.
41. Butterfield, D.A.; Owen, J.B. Lectin-affinity chromatography brain glycoproteomics and Alzheimer's disease: Insights into protein alterations consistent with the pathology and progression of this dementing disorder. *Proteomics Clin. Appl.* **2011**, *5*, 50–56.

42. Lubec, G.; Nonaka, M.; Krapfenbauer, K.; Gratzer, M.; Cairns, N.; Fountoulakis, M. Expression of the dihydropyrimidinase related protein 2 (DRP-2) in Down syndrome and Alzheimer's disease brain is downregulated at the mRNA and dysregulated at the protein level. *J. Neural. Transm. Suppl.* **1999**, *57*, 161–177.
43. Krapfenbauer, K.; Engidawork, E.; Cairns, N.; Fountoulakis, M.; Lubec, G. Aberrant expression of peroxiredoxin subtypes in neurodegenerative disorders. *Brain Res.* **2003**, *967*, 152–160.
44. Yoo, B.C.; Cairns, N.; Fountoulakis, M.; Lubec, G. Synaptosomal proteins, beta-soluble *N*-ethylmaleimidesensitive factor attachment protein (β-SNAP), γ-SNAP and synaptotagmin I in brain of patients with Down syndrome and Alzheimer's disease. *Dement. Geriatr. Cogn. Disord*. **2001**, *12*, 219–225.
45. Yoo, B.C.; Kim, S.H.; Cairns, N.; Fountoulakis, M.; Lubec, G. Deranged expression of molecular chaperones in brains of patients with Alzheimer's disease. *Biochem. Biophys. Res. Commun.* **2001**, *280*, 249–258.
46. Yoo, B.C.; Vlkolinsky, R.; Engidawork, E.; Cairns, N.; Fountoulakis, M.; Lubec, G. Differential expression of molecular chaperones in brain of patients with Down syndrome. *Electrophoresis* **2001**, *22*, 1233–1241.
47. Puchades, M.; Hansson, S.F.; Nilsson, C.L.; Andreasen, N.; Blennow, K.; Davidsson, P. Proteomic studies of potential cerebrospinal fluid protein markers for Alzheimer's disease. *Mol. Brain Res.* **2003**, *118*, 140–146.
48. Kim, S.H.; Fountoulakis, M.; Cairns, N.; Lubec, G. Protein levels of human peroxiredoxin subtypes in brains of patients with Alzheimer's disease and Down syndrome. *J. Neural. Transm. Suppl.* **2001**, *61*, 223–235.
49. Liao, L.; Cheng, D.; Wang, J.; Duong, D.M.; Losik, T.G.; Gearing, M.; Rees, H.D.; Lah, J.J.; Levey, A.I.; Peng, J. Proteomic characterization of postmortem amyloid plaques isolated by laser capture microdissection. *J. Biol. Chem.* **2004**, *279*, 37061–37068.
50. Chang, R.Y.K.; Etheridge, N.; Dodd, P.R.; Nouwens, A.S. Targeted quantitative analysis of synaptic proteins in Alzheimer's disease brain. *Neurochem. Int.* **2014**, *75*, 66–75.
51. Andreev, V.P.; Petyuk, V.A.; Brewer, H.M.; Karpievitch, Y.V.; Xie, F.; Clarke, J.; Camp, D.; Smith, R.D.; Lieberman, A.P.; Albin, R.L.; *et al.* Label-free quantitative LC-MS proteomics of Alzheimer's disease and normally aged human brains. *J. Proteome Res.* **2012**, *11*, 3053–3067.
52. Chen, S.; Lu, F.F., Seeman, P.; Liu, F. Quantitative proteomic analysis of human substantia nigra in Alzheimer's disease, Huntington's disease and multiple sclerosis. *Neurochem. Res.* **2012**, *37*, 2805–2813.
53. Zahid, S.; Khan, R.; Oellerich, M.; Ahmed, N.; Asif, A.R. Differential *S*-nitrosylation of proteins in Alzheimer's disease. *Neuroscience* **2013**, *256C*, 126–136.
54. Schmalhausen, E.V.; Nagradova, N.K.; Boschi-Muller, S.; Branlant, G.; Muronetz, V.I. Mildly oxidized GAPDH: The coupling of the dehydrogenase and acyl phosphatase activities. *FEBS Lett.* **1999**, *452*, 219–222.
55. Sunaga, K.; Takahashi, H.; Chuang, D.M.; Ishitani, R. Glyceraldehyde-3-phosphate dehydrogenase is over-expressed during apoptotic death of neuronal cultures and is recognized by a monoclonal antibody against amyloid plaques from Alzheimer's brain. *Neurosci. Lett*. **1995**, *200*, 133–136.

56. Tamaoka, A.; Endoh, R.; Shoji, S.; Takahashi, H.; Hirokawa, K.; Teplow, D.B.; Selkoe, D.J.; Mori, H. Antibodies to amyloid beta protein (Aβ) crossreact with glyceraldehyde-3-phosphate dehydrogenase (GAPDH). *Neurobiol. Aging* **1996**, *17*, 405–414.
57. Chuang, D.M.; Hough, C.; Senatorov, V.V. Glyceraldehyde-3-phosphate dehydrogenase, apoptosis, and neurodegenerative diseases. *Annu. Rev. Pharmacol. Toxicol.* **2005**, *45*, 269–290.
58. Cumming, R.C.; Schubert, D. Amyloid-beta induces disulfide bonding and aggregation of GAPDH in Alzheimer's disease. *FASEB J.* **2005**, *19*, 2060–2062.
59. Ishitani, R.; Tajima, H.; Takata, H.; Tsuchiya, K.; Kuwae, T.; Yamada, M.; Takahashi, H.; Tatton, N.A., Katsube, N. Proapoptotic protein glyceraldehyde-3-phosphate dehydrogenase: A possible site of action of antiapoptotic drugs. *Prog. Neuropsychopharmacol. Biol. Psychiatry* **2003**, *27*, 291–301.
60. Tatton, W.; Chalmers-Redman, R.; Tatton, N. Neuroprotection by deprenyl and other propargylamines: Glyceraldehyde-3-phosphate dehydrogenase rather than monoamine oxidase B. *J. Neural Transm.* **2003**, *110*, 509–515.
61. Schmitz, H.D.; Bereiter-Hahn, J. Glyceraldehyde-3-phosphate dehydrogenase associates with actin filaments in serum deprived NIH 3T3 cells only. *Cell Biol. Int.* **2002**, *26*, 155–164.
62. Waingeh, V.F.; Gustafson, C.D.; Kozliak, E.I.; Lowe, S.L.; Knull, H.R.; Thomasson, K.A. Glycolytic enzyme interactions with yeast and skeletal muscle F-actin. *Biophys. J.* **2006**, *90*, 1371–1384.
63. Oyama, R.; Yamamoto, H.; Titani, K. Glutamine synthetase, hemoglobin alphachain, and macrophage migration inhibitory factor binding to amyloid β-protein: Their identification in rat brain by a novel affinity chromatography and in Alzheimer's disease brain by immunoprecipitation. *Biochim. Biophys. Acta* **2000**, *1479*, 91–102.
64. Mawatari, K.; Segawa, M.; Masatsuka, R.; Hanawa, Y.; Iinuma, F.; Watanabe, M. Fluorimetric determination of isatin in human urine and serum by liquid chromatography postcolumn photoirradiation. *Analyst* **2001**, *126*, 33–36.
65. Igosheva, N.; Matta, S.; Glover, V. Effect of acute stress and gender on isatin in rat tissues and serum. *Physiol. Behav.* **2004**, *80*, 665–668.
66. Panova, N.G.; Zemskova, M.A.; Axenova, L.N.; Medvedev, A.E. Does isatin interact with rat brain monoamine oxidases *in vivo*? *Neurosci. Lett.* **1997**, *233*, 58–60.
67. Pandeya, S.N.; Smitha, S.; Jyoti, M.; Sridhar, S.K. Biological activities of isatin and its derivatives. *Acta Pharm.* **2005**, *55*, 27–46.
68. Zhou, Y.; Zhao, Z.Q.; Xie, J.X. Effects of isatin on rotational behavior and DA levels in caudate putamen in Parkinsonian rats. *Brain Res.* **2001**, *917*, 127–132.
69. Hamaue, N.; Minami, M.; Terado, M.; Hirafuji, M.; Endo, T.; Machida, M.; Hiroshige, T.; Ogata, A.; Tashiro, K.; Saito, H.; *et al*. Comparative study of the effects of isatin, an endogenous MAO-inhibitor, and selegiline on bradykinesia and dopamine levels in a rat model of Parkinson's disease induced by the Japanese encephalitis virus. *Neurotoxicology* **2004**, *25*, 205–213.
70. Crumeyrolle-Arias, M.; Medvedev, A.; Cardona, A.; Barritault, D.; Glover, V. *In situ* imaging of specific binding of [^{3}H]isatin in rat brain. *J. Neurochem.* **2003**, *84*, 618–620.
71. Medvedev, A.; Crumeyrolle-Arias, M.; Cardona, A.; Sandler, M.; Glover, V. Natriuretic peptide interaction with [^{3}H]isatin binding sites in rat brain. *Brain Res.* **2005**, *1042*, 119–124.

72. Medvedev, A.E.; Goodwin, D.L.; Sandler, M.; Glover, V. Efficacy of isatin analogues as antagonists of rat brain and heart atrial natriuretic peptide receptors coupled to particulate guanylate cyclase. *Biochem. Pharmacol.* **1999**, *57*, 913–915.
73. Nepali, K.; Sharma, S.; Sharma, M.; Bedi, P.M.S.; Dhar, K.L. Rational approaches, design strategies, structure activity relationship and mechanistic insights for anticancer hybrids. *Eur. J. Med. Chem.* **2014**, *77*, 422–487.
74. Campagna, F.; Catto, M.; Purgatorio, R.; Altomare, C.D.; Carotti, A.; de Stradis, A.; Palazzo, G. Synthesis and biophysical evaluation of arylhydrazono-1*H*-2-indolinones as β-amyloid aggregation inhibitors. *Eur. J. Med. Chem.* **2011**, *46*, 275–284.
75. Gonzalez, A.; Quirante, J.; Nieto, J.; Almeida, M.R.; Saraiva, M.J.; Planas, A.; Arsequell, G.; Valencia, G. Isatin derivatives, a novel class of transthyretin fibrillogenesis inhibitors. *Bioorg. Med. Chem. Lett*. **2009**, *19*, 5270–5273.
76. Zala, D.; Hinckelmann, M.V.; Yu, H.; Lyra da Cunha, M.M.; Liot, G.; Cordelieres, F.P.; Marco, S.; Saudou, F. Vesicular glycolysis provides on-board energy for fast axonal transport. *Cell* **2013**, *153*, 479–491.
77. Scopes, R.K.; Stoter, A. Purification of all glycolytic enzymes from one muscle extract. *Methods Enzymol.* **1982**, *90*, 479–490.
78. Wisniewski, J.; Zougman, A.; Nagaraj, N.; Mann, M. Universal sample preparation method for proteome analysis. *Nat. Methods* **2009**, *6*, 359–362.
79. SwissProt database. Available online: ftp://ftp.uniprot.org/pub/databases/uniprot/current_release/knowledgebase/complete/uniprot_sprot.fasta.gz (accessed on 24 December 2014).

Supplementary Information

Table S1. Identification of amyloid-binding proteins in mouse brain homogenates.

No.	Protein Name	Acc. Number [a]	Mol. Mass	Score [b]	Peptides	Localization	Function
1	Carbamoyl-phosphate synthase [ammonia], mitochondrial	CPSM_RAT	164,476	1129	15	M	6
2	Pyruvate kinase isozymes M1/M2	KPYM_RAT	57,781	706	7	C, N	1
3	Betaine—Homocysteine *S*-methyltransferase 1	BHMT1_RAT	44,948	650	2	C	6
4	Adenylate kinase 2, mitochondrial	KAD2_RAT	26,363	540	4	M	1
5	δ-1-Pyrroline-5-carboxylate dehydrogenase, mitochondrial	AL4A1_RAT	61,830	538	4	M	6
6	Actin, cytoplasmic 1	ACTB_RAT	41,710	524	3	C	2 #
7	Myosin-4	MYH4_RAT	222,741	396	4	C	2
8	3-Ketoacyl-CoA thiolase, mitochondrial	THIM_RAT	41,844	350	1	M	7
9	Hydroxyacyl-coenzyme A dehydrogenase, mitochondrial	HCDH_RAT	34,426	310	3	M	7
10	Heat shock cognate 71 kDa protein	HSP7C_RAT	70,827	305	3	C, N, S, Mel	5 #
11	ATP synthase subunit β, mitochondrial	ATPB_RAT	56,318	290	4	M	1 #
12	Calmodulin	CALM_RAT	16,827	288	1	C	2 #
13	Fructose-bisphosphate aldolase B	ALDOB_RAT	39,593	249	2	C, L, N, ER, CM	1 #
14	α-Enolase	ENOA_RAT	47,098	220	2	CM, C, Me	1 #
15	Ornithine carbamoyltransferase, mitochondrial	OTC_RAT	39,861	212	5	M	6
16	Myelin basic protein S	MBP_RAT	21,489	211	1	CM, Me	5
17	Glutathione *S*-transferase α-2	GSTA2_RAT	25,543	208	1	C, M, N	5
18	Phosphatidylethanolamine-binding protein 1	PEBP1_RAT	20,788	182	1	C, Me	4
19	Dihydropyrimidinase-related protein 2	DPYL2_RAT	62,239	177	2	C, Me, M	3 #
20	60 kDa Heat shock protein, mitochondrial	CH60_RAT	60,917	162	4	M	5
21	Glyceraldehyde-3-phosphate dehydrogenase	G3P_RAT	35,787	160	1	C, N	1 #
22	Electron transfer flavoprotein subunit α, mitochondrial	ETFA_RAT	34,929	137	3	M	1
23	Fructose-bisphosphate aldolase A	ALDOA_RAT	39,327	135	2	Me, M	1
24	ATP synthase subunit α, mitochondrial	ATPA_RAT	59,717	131	2	M	1
25	Thioredoxin-dependent peroxide reductase, mitochondrial	PRDX3_RAT	28,277	130	1	M	5
26	Elongation factor 1-α 1	EF1A1_RAT	50,082	129	2	N	3
27	Endoplasmin	ENPL_RAT	92,713	125	1	ER	5

Table S1. *Cont.*

No.	Protein Name	Acc. Number [a]	Mol. Mass	Score [b]	Peptides	Localization	Function
28	Ral GTPase-activating protein subunit α-2	RGPA2_RAT	210,200	122	1	C, N	4 #
29	Profilin-1	PROF1_RAT	14,948	119	1	C	2
30	Citrate synthase, mitochondrial	CISY_RAT	51,833	104	1	M	1 #
31	Argininosuccinate synthase	ASSY_RAT	46,467	93	1	ER, L, M, N	6
32	Keratin, type II cytoskeletal 73	K2C73_RAT	60,349	90	2	C	2
33	Peroxisomal multifunctional enzyme type 2	DHB4_RAT	79,378	89	2	P	7
34	Peroxiredoxin-1	PRDX1_RAT	22,095	87	1	C	5
35	Non-specific lipid-transfer protein	NLTP_RAT	58,775	87	4	C, M, P	2
36	Stress-70 protein, mitochondrial	GRP75_RAT	73,812	85	1	M	5 #
37	Thioredoxin, mitochondrial	THIOM_RAT	18,220	78	1	M	5
38	Enoyl-CoA hydratase, mitochondrial	ECHM_RAT	31,496	77	2	M	7
39	Citrate lyase subunit β-like protein, mitochondrial	CLYBL_RAT	37,298	74	1	M	7
40	Retinol-binding protein 4	RET4_RAT	23,205	73	1	ES	2
41	10 kDa Heat shock protein, mitochondrial	CH10_RAT	10,895	69	2	M	5
42	Aspartate aminotransferase, mitochondrial	AATM_RAT	47,284	65	2	M	6 #
43	Pyruvate carboxylase, mitochondrial	PYC_RAT	129,695	63	1	M	1 #
44	Heterogeneous nuclear ribonucleoproteins A2/B1	ROA2_RAT	37,455	63	2	N, C	3 #
45	Aspartate aminotransferase, cytoplasmic	AATC_RAT	46,400	62	1	C	6
46	78 kDa Glucose-regulated protein	GRP78_RAT	72,302	61	1	C, ER	4
47	Peroxiredoxin-2	PRDX2_RAT	21,770	59	1	C	5
48	Glutamine synthetase	GLNA_RAT	42,240	57	1	C, M	6
49	Ornithine aminotransferase, mitochondrial	OAT_RAT	48,302	56	1	M	6
50	Glutathione *S*-transferase P	GSTP1_RAT	23,424	53	1	C, M, N	5
51	ATP synthase subunit δ, mitochondrial	ATPD_RAT	17,584	45	1	M	1
52	Tubulin α-1A chain	TBA1A_RAT	50,104	43	1	C	2 #
53	Electron transfer flavoprotein subunit β	ETFB_RAT	27,670	41	1	M	1

Table S1. *Cont.*

No.	Protein Name	Acc. Number [a]	Mol. Mass	Score [b]	Peptides	Localization	Function
54	Elongation factor 2	EF2_RAT	95,223	38	1	C	3 #
55	AP-2 complex subunit mu	AP2M1_RAT	49,623	37	1	CM, Me	2 #
56	Catalase	CATA_RAT	59,719	37	1	P	5
57	Glutamate dehydrogenase 1, mitochondrial	DHE3_RAT	61,377	29	1	M	6
58	Very long-chain specific acyl-CoA dehydrogenase, mitochondrial	ACADV_RAT	70,705	29	1	M	7
59	Heat shock protein HSP 90-α	HS90A_RAT	84,762	29	1	C, Mel	5 #
60	Ubiquitin-40S ribosomal protein S27a	RS27A_RAT	17,939	29	1	C, N	5
61	Protein QN1 homolog	QN1_RAT	160,903	28	1	C, N	2
62	Ras-related protein Rab-1A	RAB1A_RAT	22,663	27	1	C, ER, E, G, Me	2
63	α-Fetoprotein	FETA_RAT	68,341	26	1	C	3
64	Trifunctional enzyme subunit β, mitochondrial	ECHB_RAT	51,382	26	1	M	7
65	Spectrin α chain, non-erythrocytic 1	SPTN1_RAT	284,462	25	2	C	2 #
66	Aldehyde dehydrogenase, mitochondrial	ALDH2_RAT	56,453	25	1	M	1
67	Phosphoglucomutase-1	PGM1_RAT	61,365	24	1	C	1
68	Arfaptin-1	ARFP1_RAT	40,754	24	1	C, G	2
69	Long-chain specific acyl-CoA dehydrogenase, mitochondrial	ACADL_RAT	47,842	23	1	M	7
70	Peroxisomal bifunctional enzyme	ECHP_RAT	78,608	23	1	P	7
71	Dimethylglycine dehydrogenase, mitochondrial	M2GD_RAT	95,987	22	1	M	6
72	Retinal dehydrogenase 1	AL1A1_RAT	54,424	21	1	C	4
73	Keratin, type I cytoskeletal 15	K1C15_RAT	48,840	20	3	C	2
74	NAD kinase domain-containing protein 1	NAKD1_RAT	48,087	20	1	M	1
75	Synaptotagmin-1	SYT1_RAT	47,369	19	1	C, Me	2 #
76	Ornithine decarboxylase antizyme 1	OAZ1_RAT	25,212	18	1	C	4
77	Protein disulfide-isomerase A5	PDIA5_RAT	59,361	17	1	ER	5
78	Regucalcin	RGN_RAT	33,368	17	1	C, N	4
79	Methylmalonate-semialdehyde dehydrogenase [acylating], mitochondrial	MMSA_RAT	57,771	17	1	M	6
80	Heterogeneous nuclear ribonucleoprotein K	HNRPK_RAT	50,944	17	1	N, C	3 #

Table S1. *Cont.*

No.	Protein Name	Acc. Number [a]	Mol. Mass	Score [b]	Peptides	Localization	Function
81	Dihydrolipoyllysine-residue succinyltransferase component of 2-oxoglutarate dehydrogenase complex, mitochondrial	ODO2_RAT	48,894	16	1	M	1
82	Acyl-protein thioesterase 1	LYPA1_RAT	24,692	16	1	C	7
83	Peroxisomal carnitine *O*-octanoyltransferase	OCTC_RAT	70,257	16	1	P	7
84	2,4-Dienoyl-CoA reductase, mitochondrial	DECR_RAT	36,110	15	1	M	7
85	Hydroxymethylglutaryl-CoA synthase, mitochondrial	HMCS2_RAT	56,876	15	1	M	7
86	Superoxide dismutase [Mn], mitochondrial	SODM_RAT	24,659	15	1	M	5 #
87	Glutathione *S*-transferase α-3	GSTA3_RAT	25,303	14	1	C, N	5 #
88	Polyadenylate-binding protein 1	PABP1_RAT	70,656	14	1	C, N, Sp	3 #
89	Putative L-aspartate dehydrogenase	ASPD_RAT	31,240	14	1	C	6

Here and in other tables letters designate extracellular space (ES), and the following intracellular compartments: C—Cytoplasm, CM—Cell membrane, E—Endosomes, ER—Endoplasmic reticulum, G—Golgi apparatus, L—Lysosomes, M—Mitochondria, Me—Membranes, Mel—Melanosomes, Mi—Microsomes, N—Nucleus, R—Ribosomes, P—Peroxisomes, S—Sarcolemma, Sp—Spliceosomes. The symbol (#) designates isatin binding proteins. [a] Entry name is the item on the ID of the sequence. This name is a useful means of identifying a sequence; [b] MASCOT search engine uses MOWSE score system as a measure of absolute probability.

Table S2. Identification of amyloid-binding proteins in mouse brain homogenate treated with 0.1 mM isatin.

No.	Protein Name	Acc. Number [a]	Mol. Mass	Score [b]	Peptides	Localization	Function
1	Carbamoyl-phosphate synthase [ammonia], mitochondrial	CPSM_RAT	164,476	587	2	M	6
2	Adenylate kinase 2, mitochondrial	KAD2_RAT	26,363	422	1	M	1
3	Heat shock 70 kDa protein 1A/1B	HSP71_RAT	70,142	421	2	C, M	5
4	Betaine—Homocysteine *S*-methyltransferase 1	BHMT1_RAT	44,948	397	2	C	6
5	δ-1-Pyrroline-5-carboxylate dehydrogenase, mitochondrial	AL4A1_RAT	61,830	350	1	M	6
6	3-Ketoacyl-CoA thiolase, mitochondrial	THIM_RAT	41,844	350	1	M	7
7	Fructose-bisphosphate aldolase B	ALDOB_RAT	39,593	286	1	C	1
8	α-Enolase	ENOA_RAT	47,098	271	1	C, N	1
9	Stress-70 protein, mitochondrial	GRP75_RAT	73,812	260	1	M	5
10	Ceruloplasmin	CERU_RAT	120,764	245	2	C	2
11	Keratin, type II cytoskeletal 73	K2C73_RAT	60,349	216	2	C	2
12	Keratin, type II cytoskeletal 8	K2C8_RAT	53,985	207	5	C	2
13	Keratin, type I cytoskeletal 15	K1C15_RAT	48,840	137	3	C	2
14	Semaphorin-3A	SEM3A_RAT	88,752	83	1	C, Me	3
15	Serine protease inhibitor A3K	SPA3K_RAT	46,532	81	1	C	3
16	Guanine nucleotide exchange factor DBS	MCF2L_RAT	129,328	68	1	C, Me	4
17	Ornithine carbamoyltransferase, mitochondrial	OTC_RAT	39,861	64	1	M	6
18	Ral GTPase-activating protein subunit α-2	RGPA2_RAT	210,200	50	1	C	4
19	Thioredoxin-dependent peroxide reductase, mitochondrial	PRDX3_RAT	28,277	46	1	M	5
20	Hydroxyacyl-coenzyme A dehydrogenase, mitochondrial	HCDH_RAT	34,426	45	1	M	7
21	Transient receptor potential cation channel subfamily M member 4	TRPM4_RAT	135,255	43	2	Me, ER, G	4
22	Glutathione *S*-transferase α-2	GSTA2_RAT	25,543	41	1	C, M, N	4

Table S2. *Cont.*

No.	Protein Name	Acc. Number [a]	Mol. Mass	Score [b]	Peptides	Localization	Function
23	Endoplasmin	ENPL_RAT	92,713	38	1	ER	5
24	Proenkephalin-A	PENK_RAT	30,912	36	1	C	4
25	Vitamin D-binding protein	VTDB_RAT	53,509	35	1	C	2
26	Glial fibrillary acidic protein	GFAP_RAT	49,927	33	3	C	2
27	Ectonucleotide pyrophosphatase/phosphodiesterase family member 5	ENPP5_RAT	54,255	32	1	Me	6
28	Xylosyltransferase 2	XYLT2_RAT	96,729	27	1	G	1

[a] Entry name is the item on the ID of the sequence. This name is a useful means of identifying a sequence;
[b] MASCOT search engine uses MOWSE score system as a measure of absolute probability.

Table S3. Identification of amyloid-binding proteins in mouse brain homogenates treated with hydrogen peroxide.

No.	Protein Name	Acc. Number [a]	Mol. Mass	Score [b]	Peptides	Localization	Function
1	Keratin, type II cytoskeletal 73	K2C73_RAT	60,349	2802	4	C	2
2	Carbamoyl-phosphate synthase [ammonia], mitochondrial	CPSM_RAT	164,476	848	6	M	6
3	Betaine—Homocysteine *S*-methyltransferase 1	BHMT1_RAT	44,948	823	2	C	6
4	Keratin, type I cytoskeletal 42	K1C42_RAT	50,182	753	5	C	2
5	Actin, cytoplasmic 1	ACTB_RAT	41,710	753	3	C	2
6	Junction plakoglobin	PLAK_RAT	81,749	676	3	C, Me	2
7	Adenylate kinase 2, mitochondrial	KAD2_RAT	26,363	556	4	M	1
8	Fructose-bisphosphate aldolase B	ALDOB_RAT	39,593	478	1	C, L, N, ER, CM	1
9	δ-1-Pyrroline-5-carboxylate dehydrogenase, mitochondrial	AL4A1_RAT	61,830	387	1	M	6
10	α-Enolase	ENOA_RAT	47,098	362	1	CM, C, Me	1
11	3-Ketoacyl-CoA thiolase, mitochondrial	THIM_RAT	41,844	354	1	M	7
12	Ornithine carbamoyltransferase, mitochondrial	OTC_RAT	39,861	272	2	M	6
13	Ubiquitin-40S ribosomal protein S27a	RS27A_RAT	17,939	244	1	C, N	5
14	Myosin-4	MYH4_RAT	222,741	226	2	C	2
15	Glutathione *S*-transferase α-2	GSTA2_RAT	25,543	202	1	C, M, N	5
16	Keratin, type II cytoskeletal 75	K2C75_RAT	58,991	192	2	C	2
17	Tropomyosin α-3 chain	TPM3_RAT	28,989	163	2	C	2

Table S3. *Cont.*

No.	Protein Name	Acc. Number [a]	Mol. Mass	Score [b]	Peptides	Localization	Function
18	60 kDa Heat shock protein, mitochondrial	CH60_RAT	60,917	161	3	M	5
19	ATP synthase subunit β, mitochondrial	ATPB_RAT	56,318	159	2	M	1
20	Hydroxyacyl-coenzyme A dehydrogenase, mitochondrial	HCDH_RAT	34,426	155	1	M	7
21	Ral GTPase-activating protein subunit α-2	RGPA2_RAT	210,200	141	1	C, N	4
22	Annexin A2	ANXA2_RAT	38,654	133	1	Me, C, Mel	2
23	ATP synthase subunit α, mitochondrial	ATPA_RAT	59,717	51	2	M	1
24	Thioredoxin-dependent peroxide reductase, mitochondrial	PRDX3_RAT	28,277	89	1	M	5
25	Elongation factor 1-α 1	EF1A1_RAT	50,082	88	2	N	3
26	Electron transfer flavoprotein subunit α, mitochondrial	ETFA_RAT	34,929	88	2	M	1
27	Tubulin α-1A chain	TBA1A_RAT	50,104	84	1	C	2
28	Retinol-binding protein 4	RET4_RAT	23,205	82	1	ES	2
29	Peroxiredoxin-1	PRDX1_RAT	22,095	71	1	C	5
30	Citrate lyase subunit β-like protein, mitochondrial	CLYBL_RAT	37,298	70	1	M	7
31	Profilin-1	PROF1_RAT	14,948	70	2	C	2
32	Endoplasmin	ENPL_RAT	92,713	67	1	ER	5
33	Thioredoxin, mitochondrial	THIOM_RAT	18,220	65	1	M	5
34	Glutathione *S*-transferase P	GSTP1_RAT	23,424	63	1	C, M, N	5
35	Peroxisomal multifunctional enzyme type 2	DHB4_RAT	79,378	63	1	P	7
36	Stress-70 protein, mitochondrial	GRP75_RAT	73,812	55	1	M	5
37	Aspartate aminotransferase, mitochondrial	AATM_RAT	47,284	54	2	M	6
38	Keratin, type I cytoskeletal 15	K1C15_RAT	48,840	52	3	C	2
39	Keratin, type II cytoskeletal 8	K2C8_RAT	53,985	48	2	C	2
40	Ornithine aminotransferase, mitochondrial	OAT_RAT	48,302	48	1	M	6
41	78 kDa glucose-regulated protein	GRP78_RAT	72,302	43	1	C, ER	4
42	Chloride intracellular channel protein 1	CLIC1_RAT	26,964	40	1	CM, C, Me, N	2
43	10 kDa Heat shock protein, mitochondrial	CH10_RAT	10,895	40	1	M	5
44	ATP synthase subunit delta, mitochondrial	ATPD_RAT	17,584	32	1	M	1

Table S3. *Cont.*

No.	Protein Name	Acc. Number [a]	Mol. Mass	Score [b]	Peptides	Localization	Function
45	2,4-Dienoyl-CoA reductase, mitochondrial	DECR_RAT	36,110	30	1	M	7
46	Dihydropyrimidinase-related protein 2	DPYL2_RAT	62,239	30	1	C, Me, M	4
47	Xylosyltransferase 2	XYLT2_RAT	96,729	30	1	ER, G, Me	1
48	Cytochrome P450 2A1	CP2A1_RAT	55,959	30	1	M	1
49	Kelch-like protein 38	KLH38_RAT	65,629	26	1	C	2
50	α-Fetoprotein	FETA_RAT	68,341	24	1	C	3
51	Myelin basic protein S	MBP_RAT	21,489	23	1	CM, Me	5
52	Calmodulin	CALM_RAT	16,827	22	2	C	2
53	Non-specific lipid-transfer protein	NLTP_RAT	58,775	22	2	C, M, P	2
54	Hydroxymethylglutaryl-CoA synthase, mitochondrial	HMCS2_RAT	56,876	22	2	M	7
55	TBC1 domain family member 14	TBC14_RAT	78,160	22	1	G	4
56	Glyceraldehyde-3-phosphate dehydrogenase	G3P_RAT	35,787	20	1	C, N	1
57	Protein piccolo	PCLO_RAT	552,376	19	1	G, Me	2
58	Synergin gamma	SYNRG_RAT	141,270	19	1	C, G, Me	2
59	Superoxide dismutase [Mn], mitochondrial	SODM_RAT	24,659	17	1	M	5
60	Hemopexin	HEMO_RAT	51,318	17	1	ES	2
61	Peroxiredoxin-2	PRDX2_RAT	21,770	16	1	C	5
62	Angiomotin-like protein 2	AMOL2_RAT	85,535	16	1	CM, G, E	4
63	Activated CDC42 kinase 1	ACK1_RAT	114,995	16	1	CM, E, Me, N	2
64	Probable G-protein coupled receptor 19	GPR19_RAT	47,603	15	1	CM, Me	4
65	Granulins	GRN_RAT	63,325	15	1	ES	3
66	Furin	FURIN_RAT	86,599	15	1	CM, Me, G	3
67	Enoyl-CoA hydratase, mitochondrial	ECHM_RAT	31,496	15	1	M	7
68	Cullin-associated NEDD8-dissociated protein 2	CAND2_RAT	139,585	14	1	N	3
69	Citrate synthase, mitochondrial	CISY_RAT	51,833	14	1	M	1
70	Heat shock protein HSP 90-α	HS90A_RAT	84,762	13	1	C, Mel	5

[a] Entry name is the item on the ID of the sequence. This name is a useful means of identifying a sequence;

[b] MASCOT search engine uses MOWSE score system as a measure of absolute probability.

Table 4. Identification of amyloid-binding proteins in mouse brain homogenates treated with hydrogen peroxide in the presence of 0.1 mM isatin.

No.	Protein Name	Acc. Number [a]	Mol. Mass	Score [b]	Peptides	Localization	Function
1	Dihydropyrimidinase-related protein 2	DPYL2_RAT	62,239	627	1	C, Me, M	3
2	Betaine—Homocysteine *S*-methyltransferase 1	BHMT1_RAT	44,948	534	4	C	6
3	Cytosolic 10-formyltetrahydrofolate dehydrogenase	AL1L1_RAT	98,812	387	8	C	1
4	Keratin, type II cytoskeletal 73	K2C73_RAT	60,349	345	3	C	2
5	78 kDa Glucose-regulated protein	GRP78_RAT	72,302	302	6	ER	5
6	Tubulin α-1A chain	TBA1A_RAT	50,104	261	4	C	2
7	Clathrin heavy chain 1	CLH_RAT	191,477	240	6	C	2
8	Glial fibrillary acidic protein	GFAP_RAT	49,927	240	2	C	2
9	Actin, cytoplasmic 1	ACTB_RAT	41,710	231	5	C	2
10	Heat shock cognate 71 kDa protein	HSP7C_RAT	70,827	213	7	C, M	5
11	Keratin, type II cytoskeletal 8	K2C8_RAT	53,985	207	5	C	2
12	Dynamin-1	DYN1_RAT	97,234	191	6	C	2
13	Tubulin β-2A chain	TBB2A_RAT	49,875	179	3	C	2
14	Annexin A6	ANXA6_RAT	75,706	152	4	C, Mel	2
15	Tubulin α-4A chain	TBA4A_RAT	49,892	149	4	C	2
16	Ubiquitin-40S ribosomal protein S27a	RS27A_RAT	17,939	133	2	C, N, R	3
17	Myosin-4	MYH4_RAT	222,741	129	2	C	2
18	Peroxiredoxin-1	PRDX1_RAT	22,095	129	3	C	5
19	Transitional endoplasmic reticulum ATPase	TERA_RAT	89,293	125	3	C, N, ER	2
20	Heterogeneous nuclear ribonucleoprotein A3	ROA3_RAT	39,628	125	2	N, C	3
21	Glutathione *S*-transferase P	GSTP1_RAT	23,424	116	1	C, M, N	5
22	Calmodulin	CALM_RAT	16,827	116	1	C	4
23	Synapsin-2	SYN2_RAT	63,417	106	2	C	4
24	Keratin, type I cytoskeletal 42	K1C42_RAT	50,182	105	4	C	2
25	Cytochrome b5	CYB5_RAT	15,346	100	3	ER, Me, Mi	1

Table S4. *Cont.*

No.	Protein Name	Acc. Number [a]	Mol. Mass	Score [b]	Peptides	Localization	Function
26	Activated RNA polymerase II transcriptional coactivator p15	TCP4_RAT	14,432	91	2	N	3
27	Catalase	CATA_RAT	59,719	79	3	P	5
28	Polyadenylate-binding protein 1	PABP1_RAT	70,656	75	2	C, N, Sp	3
29	Neurofascin	NFASC_RAT	137,918	69	2	CM, Me	5
30	Glutamate dehydrogenase 1, mitochondrial	DHE3_RAT	61,377	68	4	M	6
31	Arginase-1	ARGI1_RAT	34,951	55	2	C	6
32	Creatine kinase U-type, mitochondrial	KCRU_RAT	46,999	54	1	M	1
33	Spectrin α chain, non-erythrocytic 1	SPTN1_RAT	284,462	50	4	C	2
34	Vesicle-fusing ATPase	NSF_RAT	82,600	47	1	C	2
35	Heat shock protein HSP 90-α	HS90A_RAT	84,762	45	1	C, Me	5
36	Heterogeneous nuclear ribonucleoproteins A2/B1	ROA2_RAT	37,455	43	2	N, C, R, Sp	3
37	Fructose-bisphosphate aldolase B	ALDOB_RAT	39,593	41	1	C, L, N, ER, CM	1
38	ATP synthase subunit β, mitochondrial	ATPB_RAT	56,318	39	2	M	1
39	Peroxiredoxin-2	PRDX2_RAT	21,770	38	1	C	5
40	Malate dehydrogenase, cytoplasmic	MDHC_RAT	36,460	38	2	C	1
41	Elongation factor 1-α 1	EF1A1_RAT	50,082	38	1	N, C	3
42	Calcium/calmodulin-dependent protein kinase type II subunit α	KCC2A_RAT	54,081	31	1	Me, CM	4
43	Pyruvate kinase isozymes M1/M2	KPYM_RAT	57,781	30	1	C, N	1
44	Myelin basic protein S	MBP_RAT	21,489	28	1	Me, CM	4
45	Stress-70 protein, mitochondrial	GRP75_RAT	73,812	26	1	M, N	5
46	Glutamine synthetase	GLNA_RAT	42,240	26	2	C, M	6
47	Heterogeneous nuclear ribonucleoprotein H2	HNRH2_RAT	49,262	24	2	C, N, R	3
48	Histone H3.1	H31_RAT	15,394	20	1	N	3

Table S4. *Cont.*

No.	Protein Name	Acc. Number [a]	Mol. Mass	Score [b]	Peptides	Localization	Function
49	Carbamoyl-phosphate synthase [ammonia], mitochondrial	CPSM_RAT	164,476	19	1	M	6
50	Ras-related protein Rab-4B	RAB4B_RAT	23,614	18	1	M, CM	4
51	Endoplasmin	ENPL_RAT	92,713	17	1	ER	5
52	Keratin, type II cytoskeletal 72	K2C72_RAT	56,816	17	1	C	2
53	Dihydrolipoyllysine-residue acetyltransferase component of pyruvate dehydrogenase complex, mitochondrial	ODP2_RAT	67,123	16	1	M	1
54	Histone H2B type 1-A	H2B1A_RAT	14,216	16	1	N	3
55	14-3-3 protein ζ/δ	1433Z_RAT	27,754	15	1	C, N, M, Me	3
56	Uricase	URIC_RAT	34,912	15	1	P	6
57	Kelch-like protein 38	KLH38_RAT	65,629	15	1	C, G	5
58	Glutathione *S*-transferase Yb-3	GSTM4_RAT	25,664	14	1	C	5
59	Isocitrate dehydrogenase [NADP] cytoplasmic OS	IDHC_RAT	46,705	13	1	C	1

[a] Entry name is the item on the ID of the sequence. This name is a useful means of identifying a sequence;

[b] MASCOT search engine uses MOWSE score system as a measure of absolute probability.